LAWRENCE
LIVERMORE
NATIONAL
LABORATORY

LLNL-CONF-613592

Image Processing And Control Of A Programmable Spatial Light Modulator For Spatial Beam Shaping

A. A. S. Awwal, C. Orth, E. Tse, J. Matone, M. Paul, C. Hardy, G. Brunton, M. Hermann, S. Yang, J. M. DiNicola, M. Rever, S. Dixit, P. Wegner, J. Heebner

January 28, 2013

SPIE Photonics West 2013
San Francisco, CA, United States
February 3, 2013 through February 7, 2013

Disclaimer

Image processing and control of a programmable spatial light modulator for spatial beam shaping

Abdul A. S. Awwal, Charles Orth, Eddy Tse, JoAnn Matone, Mitanu Paul, Carla Hardy, Gordon Brunton, Mark Hermann, Steve Yang, J.M. DiNicola, Matt Rever, Sham Dixit, Paul Wegner and John Heebner

Integrated Computer Control System, National Ignition Facility
Computer Engineering division
Lawrence Livermore National Laboratory, Livermore, CA. 94551
E-mail: awwal1@llnl.gov

ABSTRACT

Programmable spatial shapers using liquid-crystal-based spatial-light-modulators in the National Ignition Facility lasers enable spatial shaping of the beam profile so that power delivered to the target can be maximized while maintaining system longevity. Programmable spatial shapers achieve three objectives: Introduce obscurations shadowing isolated flaws on downstream optical elements that could otherwise be affected by high fluence laser illumination; Spatial shaping to reduce beam peak-to-mean fluence variations to allow the laser to operate at higher powers so that maximum power can be delivered to the target; And finally gradually exposing the optical regions that have never seen laser light because they have always had shadowing from a blocker that is no longer needed. In this paper, we describe the control and image processing algorithms that determine beam shaping and verification of the beam profile. Calibration and transmittance mapping essential elements of controlling the PSS are described along with spatially nonlinear response of the device such as scale and rotation.

Key word: control systems, laser alignment, beam shaping, liquid crystal device, spatial light modulator

1. INTRODUCTION

Inertial confinement fusion research at the National Ignition Facility (NIF) of the Lawrence Livermore National Laboratory, is performed on a 192-beam, 1.8 megajoule, 500-terawatt, ultraviolet, laser system [1-3]. The key functions of the NIF laser such as specifying pulse shape, alignment, amplification and beam control are managed by the integrated computer control system (ICCS) in order to produce proper timing, high-energy density and pressure leading to a controlled fusion reaction [4-7]. ICCS divides alignment, optics inspection and shot planning, etc. into various subsystems. While the automatic alignment (AA) system analyzes beam images to determine beam centering to perform optical alignment, the optics inspection (OI) system, is used to identify flaws of different sizes on various optical elements in the beam path and track them over time.

One of the challenges of operating NIF is to maintain the high quality of the optical elements that are subjected to repetitive laser shots. Exposure to high-fluence laser light can cause some optical flaws to grow over time and impact performance. The programmable spatial shaper (PSS) based on liquid-crystal spatial light modulators (SLM) was designed and implemented within the NIF laser to introduce arbitrarily shaped obscurations that act to reduce laser irradiation around selected flaw sites [8]. The OI system and Laser Performance Operations Model (LPOM) [9] supply the flaw site information, while the PSS system provides “blockers” that cast a shadow in the beam effectively reducing flaw irradiation exposure. A second objective of this spatial shaper, in addition to deploying blockers, is to reduce beam

peak-to-mean fluence variations to allow the laser to operate at higher powers so that most of the energy can be delivered to the target, while being in the machine safety limit.

To control the operation of the PSS module, an integrated computer control subsystem was developed. The PSS control system controls the creation the blockers of various sizes, gray levels and overall beam spatial shape as specified by LPOM and verifying that the blockers satisfy location, gray level and shape. An image of the beam imprinted with the specified blockers is passed to the image processing module, which verifies that the PSS blocker positions and characteristics match the desired specifications. A secondary challenge is to characterize the PSS in terms of coordinate mapping and gray level to transmittance mapping. In this paper, we describe the control and associated image processing of the PSS subsystem. Next we briefly describe the optical subsystem [8].

2. PSS: OPTICAL SYSTEM

The purpose of the PSS system is to control the irradiance of flaws on high-fluence optics, which is accomplished by creating shadows by PSS blockers introduced in the low-fluence region of the beam path, known as the pre-amplifier module or PAM. Before the PSS, shadows in the PAM were achieved by chrome masks, which were inflexible and incapable of meeting the demands of real-time operation. To increase operational flexibility, a programmable method of generating blockers was sought. Commercially available pixelated SLMs were unattractive because of problems with diffraction, wavefront and spectral distortions. An optically-addressable transmissive light valve technology was therefore selected. As shown in Figure 1, the programmable blockers were incorporated in the PAM with a goal to project the blockers downstream to shadow flaws in the high-fluence region of the final optics assembly.

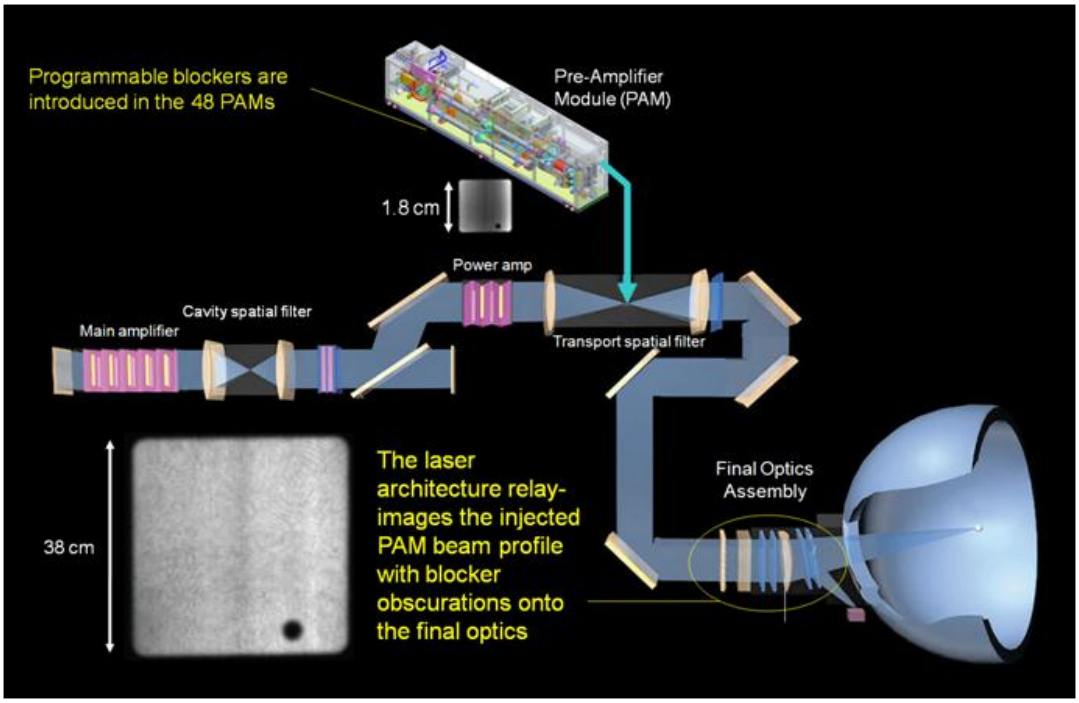

Figure 1. A diagram showing the relative location of the PSS unit (in the PAM) compared to the overall beam path, the final optics assembly and the target chamber.

The spatial beam modulation is accomplished in a cascaded two-step process. In the first step, the desired bitmapped blocker image is imprinted onto an incoherent blue LED light, using a standard 1920 x 1080 pixel Liquid Crystal on Silicon (LCoS) modulator. The incoherent beam imprints the information on the write-side of an optically addressed

light valve (OALV), which consists of a large, single pixel twisted nematic liquid crystal cell in series with a layer of photoconductive Bismuth Silicon Oxide (BSO). The encoded bit-mapped pattern alters the spatial voltage around a fixed bias to the liquid crystal layer. When the OALV is read by the 1053 nm coherent laser beam, its polarization is modulated by this voltage pattern. A subsequent polarizer converts the polarization modulation into amplitude modulation. Consequently, apodized patterns free from spurious pixelization artifacts are generated by this second stage, which transfers the desired blockers, gray level and beam profile to the coherent main laser beam [8].

3. CONTROL OF PSS

The position, shape and transmission of the obscurations must be carefully verified prior to high-fluence operations. System performance would be adversely affected by an improperly placed blocker. Furthermore, the spatially varying nonlinear response of the device must be incorporated by calibrating the device at multiple sub-image locations. The operation of the PSS must thus be performed in a sequence of three steps: 1) a calibration is performed to match the position, size and transmittance of the obscurations with respect to the deployed beam blockers; 2) the calibration constants found in step 1 is used to deploy the actual blockers to block the flaw sites. In both cases, image processing algorithms are used to perform detection and estimation of the imposed blocker centroid positions and transmittance; 3) verification is performed to ensure blockers are properly deployed with respect to position, size, and contrast.

3.1 PSS Calibration

The PSS system calibration is critical to the accurate placement and scaling of blocker obscurations. All blocker locations specified within the system are specified relative to the input sensor package (ISP)[10] CCD image plane (640x480 pixels) as shown in Figure 2. PSS System calibration provides the PSS controller with the factors necessary to translate between the ISP CCD pixel locations and the LCoS SLM pixel locations where the blockers are rendered. Calibration consists of two main phases, commissioning and operation.

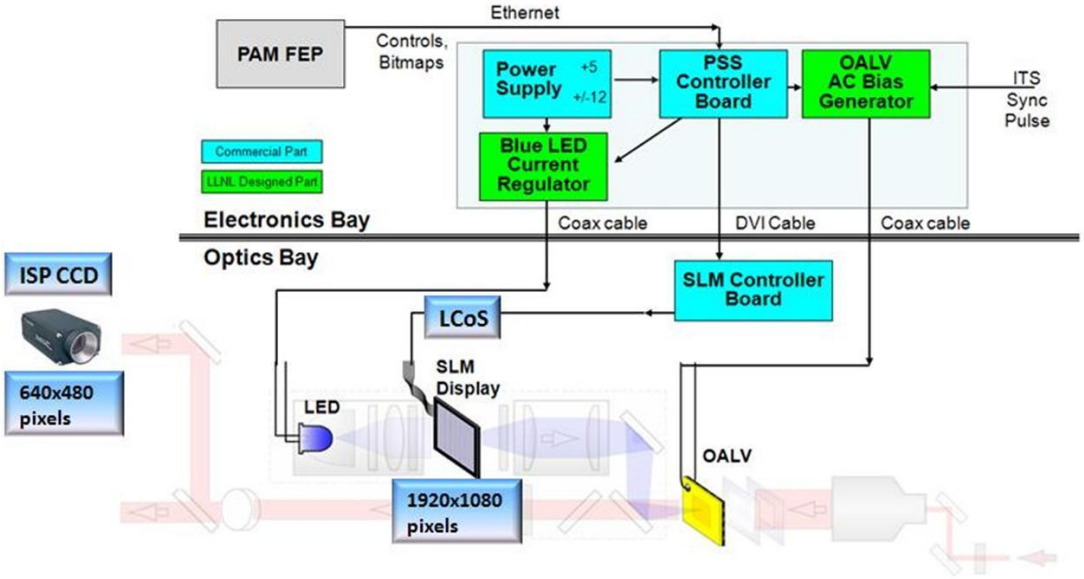

Figure 2. PSS Control Point Overview. The "PAM FEP" at top is the pre-amplifier module front-end processor.

3.1.1. Calibration during device commissioning

The PSS system control uses two image planes − the LCoS SLM display (1920x1080 pixels) on which the blocker obscurations are rendered, and the ISP CCD camera (640x480 pixels) that is used to verify that blocker obscurations are correctly located and have the requested diameter. These two image planes have independent resolutions and offsets. Commissioning calibration grossly calibrates the deployment (LCoS) image plane to the verification (ISP) image plane by measuring both the x/y offset and the scaling factor required to transform between the two planes. These calibration factors are unique for each PSS system and are generally only measured and recorded during the installation of each PSS system or when maintenance is performed on the system. The accuracy of these gross factors is not particularly critical as any minor variances are removed by the automated fine operational calibration performed during deployment operation as part of every NIF shot cycle.

3.1.2. Operational Calibration: position, scale and magnification

As the NIF optical beamlines are aligned on every shot cycle, small variances in PSS alignment can occur between shots. To address these variances the PSS system requires two operational calibrations during each shot cycle to ensure the accuracy of blocker deployments, and thus minimize the laser energy exposure on the corresponding final optic flaw locations. The operational calibration is divided into two steps: 1) positional calibration 2) gray level calibration.

The commissioning calibration activity provides the offset and scale factors necessary to place blockers in approximate location required for a shot. Due to several optical and system factors, spatial distortions exist across the entire beam aperture. The first operational calibration activity involves refining these gross factors, accomplished by the deployment of a five-by-five grid of blockers to measure these distortions at specified discrete locations across the beam aperture. Using image processing routines to accurately estimate the position and diameter of these blockers, the calibration routine automatically adjusts the deployed blocker grid locations and diameters until both are within tolerance of the requested settings. This blocker grid is shown in Figure 3.

As all blocker locations are specified in relation to a static fiducial reference located at the center of the square cutout on the left alignment “wing mask”, the final operational calibration uses image processing to calculate the offset from the image origin to the center of the fiducial.

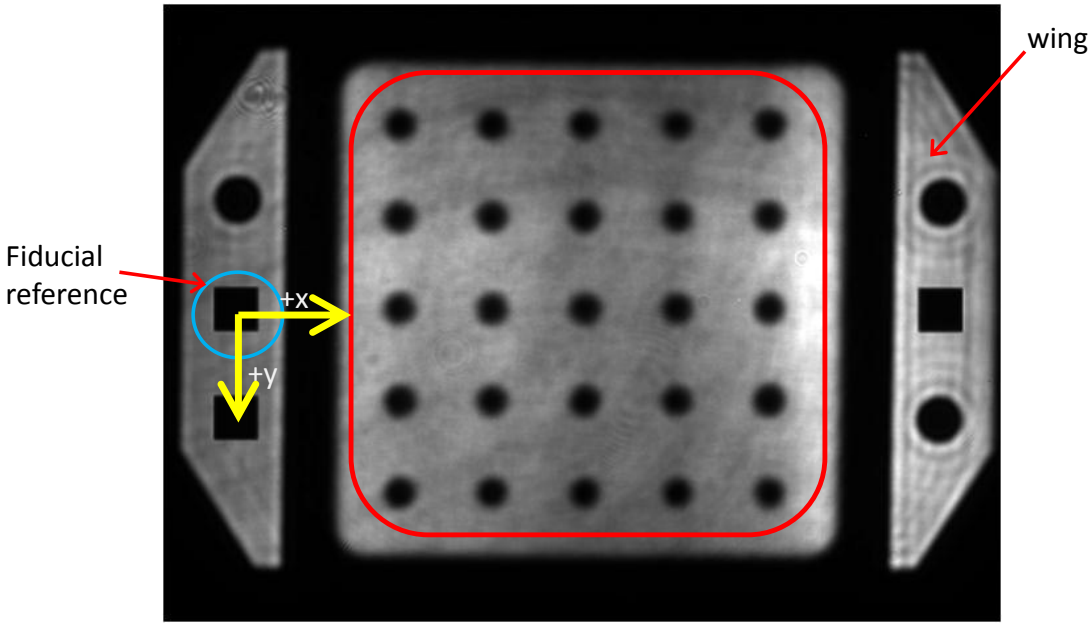

Figure 3. PSS Operational Calibration Components.

Once commissioning and operational calibrations are complete, the PSS controller stores all calibration factors that will then be used for the deployment of the blockers required for a specific shot. To recap, the factors recorded during the calibration activities are:

a) Displacement - ISP to LCoS offset factors (x, y)
b) Scale/magnification - ISP to LCoS scale factor
c) Fine scale - Fine offset and diameter correction factors for each calibration grid location
d) Origin - Fiducial reference offset.

Calibration is performed on the PSS system as a predecessor to the blocker deployment, rather than incorporating the calibration activity into the blocker deployment activity, to avoid issues encountered when attempting to perform 'on-the-fly' calibration of overlapping blockers and blockers that may intersect the edge of the beam aperture. Performing the calibration up front has proven to increase the robustness of the PSS system because it is unaffected by arbitrary shot blocker locations (which due to the optics inspection and analysis processing can include locations almost entirely outside the beam aperture).

3.1.3. Gray level Calibration

In order to deploy a blocker to have a certain transmittance (other than 0% or highest transmittance) one needs to characterize the PSS system to capture its gray level to transmittance modulation characteristics. This transmittance calibration is the last step in the calibration process. This is accomplished by deploying 25 blockers as shown in Fig. 3 whose gray levels are set every 15 counts from 0 to 255. The transmittance at the center of these 25 blockers is then measured. The transmittance is defined as the ratio of the mean intensity at the center of each blocker within a defined area of $m \times m$ pixels to the mean intensity of the same area in a reference image defined as the image without any blockers (i.e., where the SLM is set at its maximum possible transmittance). The plot these transmittance measurements as shown in Fig. 4 are named S-curves, which does exhibit a variation of the device transmission characteristics at different blocker locations. When a gray blocker is deployed, the specified transmittance is achieved

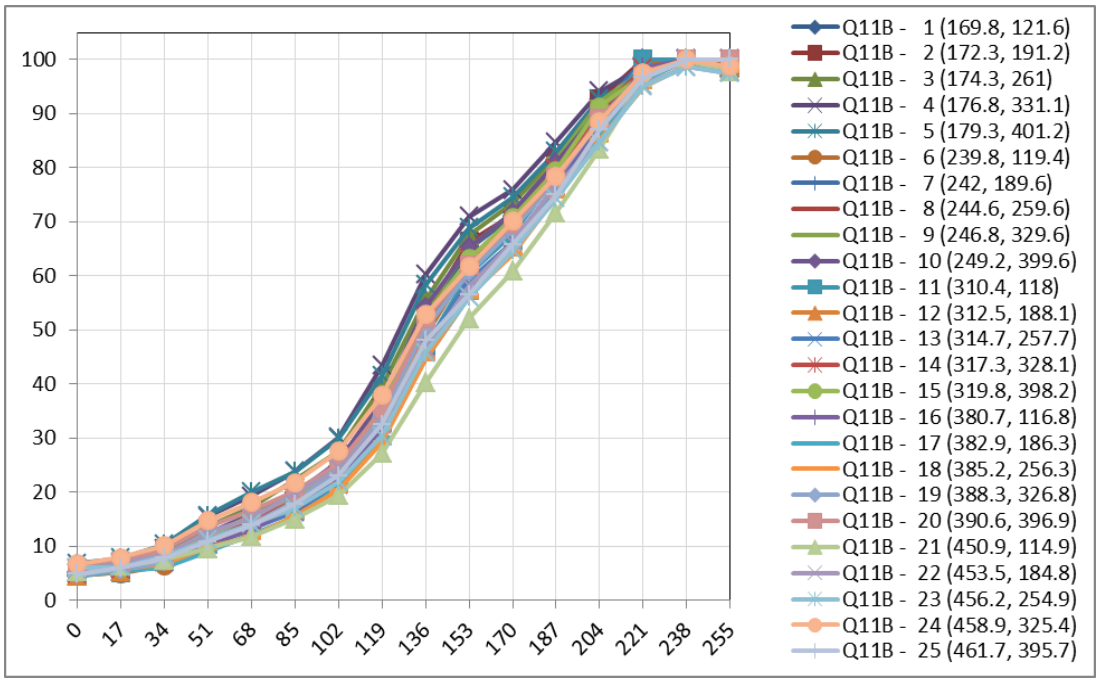

Figure 4. The 25 S-curves for quad Q11B showing transmittance as a function of gray level.

by an inverse truth table look up performed by using these graphs depending on the location of the blocker. Any blockers that are placed in-between these grid points uses a weighted S-curve of the four nearest neighbors.

3.2 Specifying the beam shaper

PSS blockers are deployed and verified for each NIF shot cycle. The quantity and location of blockers deployed on each beam depends on two factors: 1) the location and severity of the optic flaw that exists in the downstream beamline optic, and 2) the energy requirements of the shot experiment. Since the blockers are specified in ISP co-ordinates, they must be transformed into the LCOS coordinates prior to deployment. The transformation details which include both the coordinate transformation and magnification of blocker size are explained in details in Ref. [11]. Mainly three types of spatial shapes are deployed: black blockers, gray blockers and the spatial shaper.

3.2.1 Black blockers

Depending on the position and size of a flaw on a downstream optic, two main types of blockers may be deployed. Isolated flaws could be mitigated by a blocker of a single radius at that particular location. When the size of the flaw is bigger or extends to a certain length, multiple overlapping blockers may be deployed. Figure 5 shows some typical black blockers. Due to apodization, a deployed blocker (shown in red) may measure to be slightly bigger (shown in green).

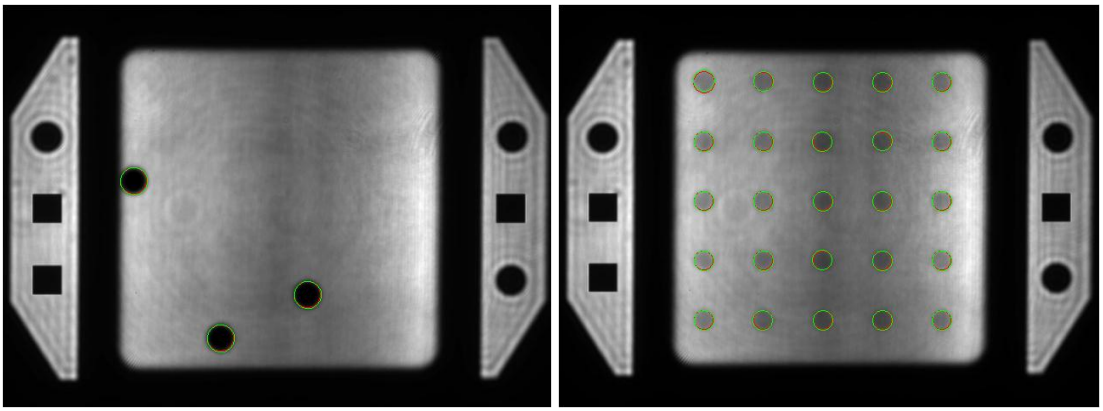

Figure 5. Three black blockers (left) and Gray blockers with 70% transmission (right); detected locations in green and desired locations in red.

3.2.2 Gray blockers

The gray blockers usually have a specified nonzero transmission. Once an optic has changed, a blocker may not be necessary, however, the power to the downstream optics need to be gradually increased as it has not been exposed to high fluence due to the presence of a blocker. Gray blockers allow the flexibility to increase the power to an optic when a blocker is no longer needed by gradually conditioning the unexposed region of the optics through incremental power exposure, thus reducing the power loss and boosting the fluence delivered to the target. Each blocker deployment must specify the position, diameter and transmission, which for the black blocker is 0. A 5x5 gray blocker grid with 70% transmission gray level is shown above. Note that closeness of the red/green circle indicates the proximity of the deployed and detected blocker positions.

3.2.3 Spatial shaper

The 192 NIF beams are organized into forty eight quads. All quads are spatially shaped by the same static chrome-on-glass mask. However, due to quad-to-quad variation in amplifier gain profile, different quads exhibit different beam profiles. These nonuniformities result in high fluence peaks, which may initiate or enhance a flaw in the optics, and may limit the maximum power at which the laser operates. The objective of the beam shaping is to provide a flat beam profile so that high fluence peaks are reduced. This is done by the programmable shaper which implements a transmission profile that minimizes beam peak-to-mean fluence variations to allow the laser to operate at higher powers. By reducing high fluence peaks the machine safety margin for high power operations can be vastly increased and possible energy that can be delivered to the target maximized. The PSS system is required to program the SLM to

produce this specified spatial shape. In section 4, we describe how this spatial shape is implemented and verified. The control panel for the PSS for spatial shaper operation is displayed in Figure 6.

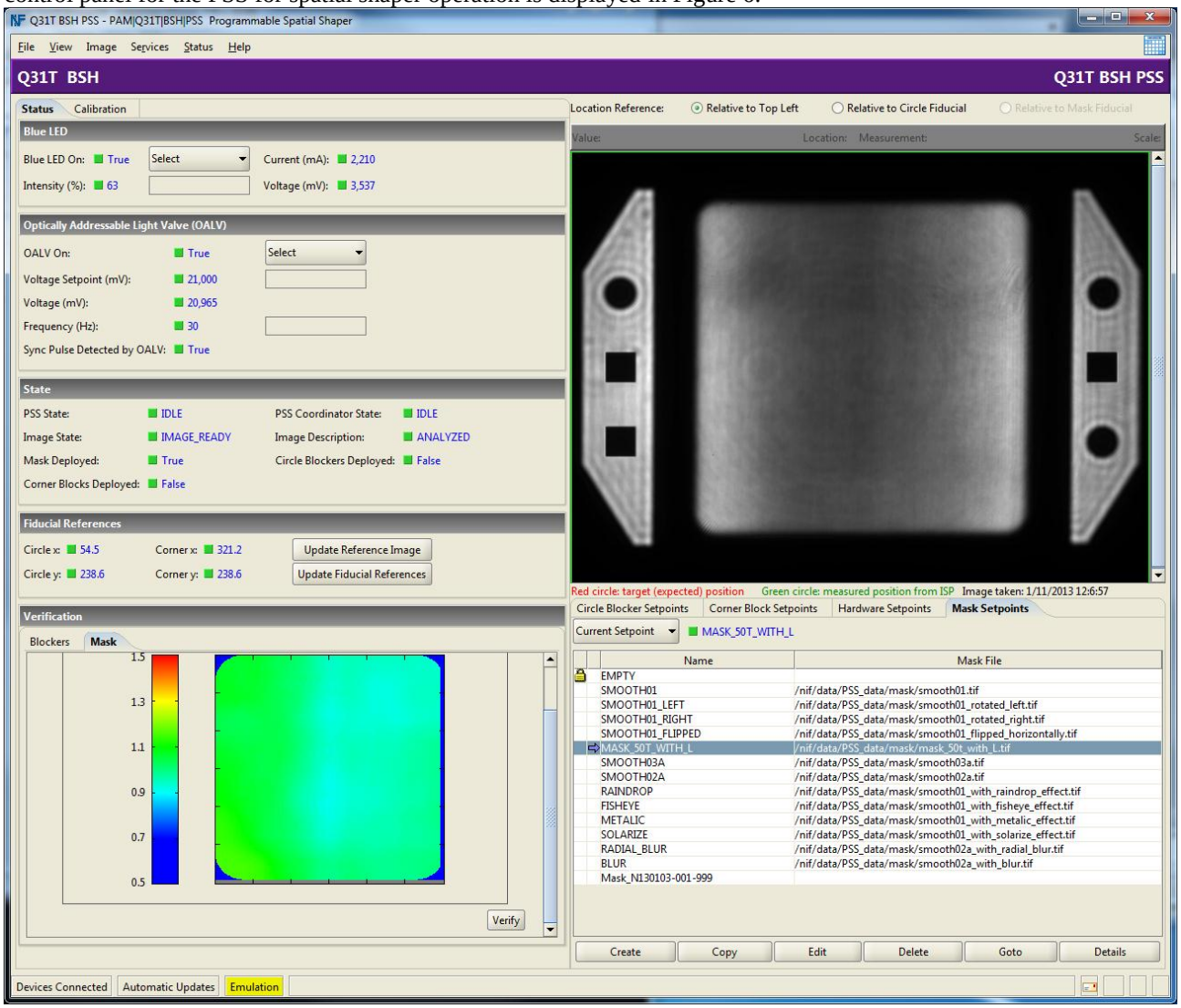

Figure 6. The spatial shaper graphical user interface

3.3 Validation

For a blocker to be verified, three blocker properties are confirmed: location, size and transmission. These properties are considered acceptable if the deviation of the detected parameters from the requirements is within a certain range. If the location is more than three pixels away from the specified position, then it is considered to have failed. If the size of the detected blocker is bigger than specified then it is acceptable; if smaller, it is not acceptable. The transmission is accepted if it is less than a certain threshold. For whole beam shaping, the rms of the normalized difference is used as a verification criterion.

4. IMAGE PROCESSING

Once the control system imprints the blockers on the SLM, the modulated PSS image is captured by an input sensor package (ISP) camera and sent to the automated alignment image processing unit. Depending on the three different types of PSS shapes deployed, three different functionalities are accomplished by three different AA image processing

units: calibration, circle-blockers and spatial shaper units. For the circle and calibration blockers, matched filtering is used to detect their position.

4.1 Matched filtering

Matched filtering (MF) [12,13] has demonstrated remarkable success in determining the location of distinctly shaped beam fiducials [14-16]. One of the chief advantages of MF is that it can be applied to the analog domain image without performing extensive preprocessing. Matched filtering techniques rely on the fact that the position of a fiducial is the location of the highest correlation peak, when matched with a template representing the fiducial.

The matched filtering algorithm utilized here is performed in the frequency domain using a filter defined by

$$H_{CMF}(U_x,U_y) = F^*(U_x,U_y) = \left|F(U_x,U_y)\right| \exp(-j\Phi(U_x,U_y)) \tag{4}$$

Where, U_x,U_y, are the spatial frequency domain variables and Φ is the phase of the Fourier transform of the to-be-searched pattern function $f(x,y)$ as denoted by:

$$F(U_x,U_y) = \left|F(U_x,U_y)\right| \exp(\, j\Phi(U_x,U_y)) \tag{5}$$

The product of Equations (4) and (5) produces the correlation in the Fourier domain. Then the inverse Fourier transform of the product produces the auto- or cross-correlation. When (5) is replaced by the Fourier transform of the image containing template, cross-correlation between the template and the image results. The performance of the matched filter can be further enhanced by extracting the edge [15] of the image and using the edge of the to-be-detected features as the filter. This has an equivalent effect of high-pass filtering the correlation output, thus increasing the sharpness of the peaks [17,18]. The position of the object can be found from the position of the cross correlation peak, autocorrelation peak, and the center of the templates as shown in Eqs. (6) and (7).

$$x_{pos} = x_{cross} - x_{auto} + x_c \tag{6}$$

$$y_{pos} = y_{cross} - y_{auto} + y_c \tag{7}$$

In these equations, (x_{pos},y_{pos}) is the to-be-determined position of the pattern in the image plane, (x_{auto},y_{auto}) is the position of the template autocorrelation peaks and (x_{cross},y_{cross}) is the position of the cross correlation peak. The position of the cross-correlation peak was estimated using a polynomial fit of second order to the correlation peak. The center of the template, (x_c,y_c) is calculated on-the-fly. The (x_{auto},y_{auto}) is the center of the image plane. The above formula allows the template to be placed anywhere in the image, however, if it is centered then the last two terms cancel each-other simplifying the calculation.

4.2 Detecting the calibration blockers

Calibration is a closed loop process, whereby the deployed and measured locations are matched over several iterations by adjusting the calibration parameters. For calibration blockers, such as shown in Figure 3, the approximate blocker position is determined by binarization (converting to a binary image) and centroiding as elaborated next. Because the PAM image is modulated by a quadratic mask, a global statistics-based binarization does not work. After removing the wings, the PAM image is therefore divided by the reference image to convert it into a uniform-intensity beam. After removing some of the artifacts of division, the resulting image is inverted and binarized, and approximate centroid

locations are calculated for blocker locations. In the initial steps of calibration, some of the blockers may be located outside the beam or be partially truncated, which are missed in the centroiding process. In those cases, the missing blockers are detected by comparing the detected circle locations with the supplied input locations and replacing the missing ones with the corresponding input location. Starting with these locations and approximate sizes, a matched filter is used to refine the radius for each circle on the edge-detected binary sub-image. Gradually as the scaling parameters are adjusted in the subsequent iterations, most of the blockers fall completely inside the beam. As a final check, the distances between the various blockers are measured in order to remove spurious misdetected features as blockers. The various steps of image processing [19] of the calibration blockers are depicted in the block diagram of Figure 7.

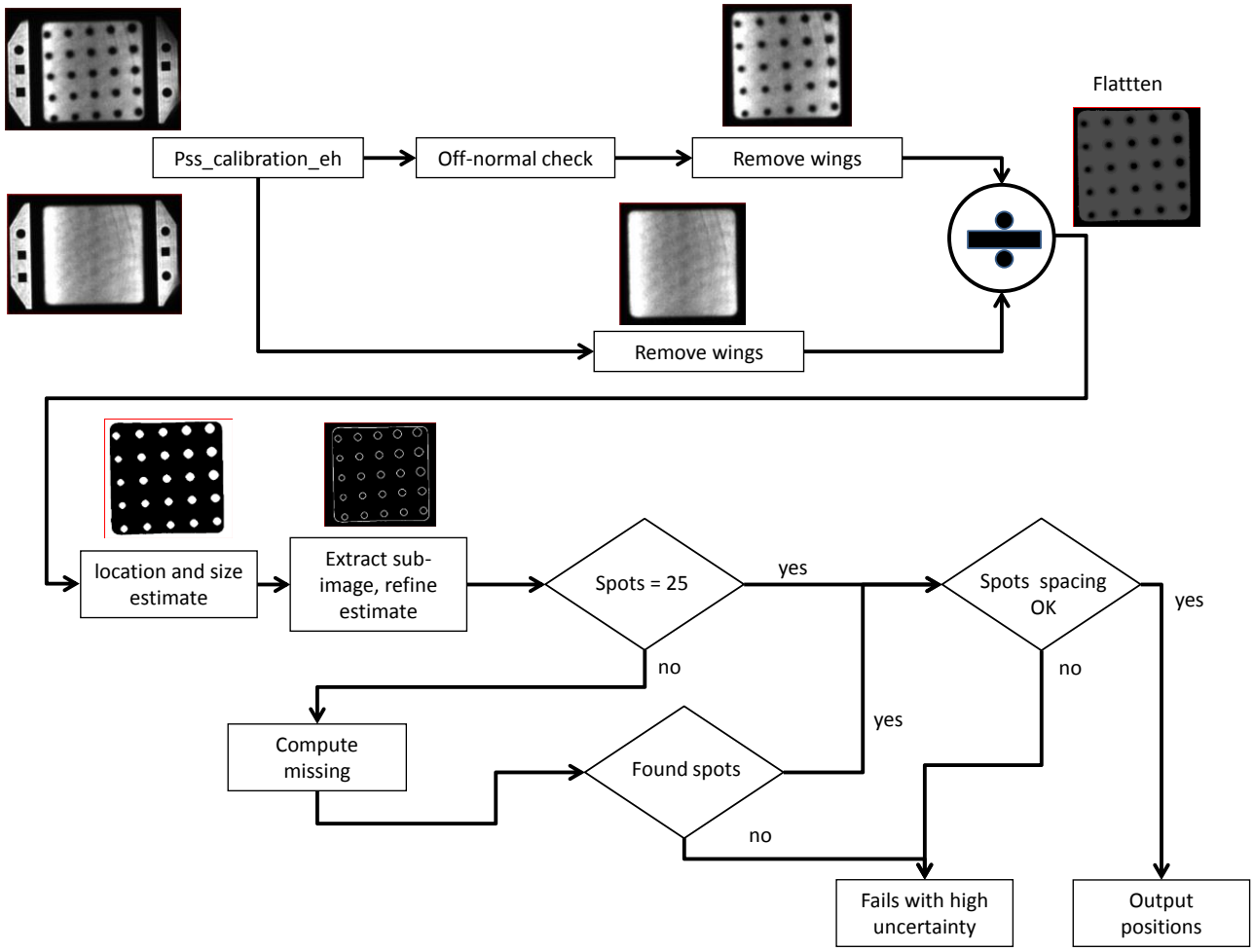

Figure 7. Block diagram of PSS calibration blocker detection algorithm.

4.3 Detecting Gray or black blockers

Finding blocker positions in calibration and those in deployment have several distinctions. In calibration, blockers have high contrast, but a deployed blocker may have a higher transmission and also may be overlapped with another blocker. Both of these effects tend to reduce the contrast and edge features and make centroiding less effective. Once the PSS system has been calibrated, we expect to find the blockers very close to where they are deployed. After flattening, a sub-image is formed by segmenting the image around the supplied input blocker position with an offset that defines the size of each sub-image. In the case of calibration, the blockers are expected to be shifted, so the goal in that case is to find their location without using any prior knowledge. However, in the deployed case, use of supplied positions is useful in reducing the ambiguity especially in the case of overlapped or low-contrast gray blockers.

The use of a subimage for processing the image speeds up the processing time tremendously. From each subimage, the local maxima and minima are calculated and then the subimage is binarized halfway between the two extremas to get the measurement for the size and location of the blockers. The matched filter is used on individual edges detected in the binarized sub-images to refine the radius and the position. Due to apodization and subsequent binarization, the radii of the circle blockers may differ from those specified. In addition, when overlapped circles are formed, the edges of the circles that are in-between two circles are not easily found; in that case, the input circle radius and location are chosen if the transmission of the location is within a tolerance of what is specified. The overlapped internal circles are refined by matched filtering if more than half of the edges remain intact.

After the location of each circle is determined, the unprocessed reference and beam subimages are used to estimate the transmittance values as a ratio of the mean values within a region of interest (ROI). The ROI used for this is an externally controllable pixel region that is a database parameter specified as a given number of pixels. Once the location and transmittance of each blocker are calculated, they are compared against the input specifications. If the deviation is under 3 pixels and the transmittance is within 30%, it is accepted. However, we found during PSS development that there would be cases when the failure is due to a distance of say 3.1 pixels. In order to minimize frequent failures for such cases, it was decided to check the location of the original blocker and if it is sufficiently dark (i.e. near 0 transmission), then change the location of the found blocker to that of the input location, thus indicating that this blocker has covered the desired location. If it is not sufficiently dark, then we keep the found distance and let the PSS fail. In case of failure due to distance or transmittance, the blockers may be redeployed or a new calibration may be performed. Redeployment may have a draw back if the blocker was at a distance much greater than 3 pixels, so a new calibration may be required. When the blocker is deployed at an area outside the beam, a special processing is done so that it does not flag a 100% transmittance (as the ratio of background mean values).

4.4 Deploying and verifying spatial blockers

Overall correction of a 2D beam to a specified prefigured spatial shape can be accomplished by multiplying by a 2D factor that minimizes beam fluctuations. This factor is estimated from four output beams collected at the output sensor package (OSP). LPOM forms a 2D PSS correction by minimizing the peak/mean on four OSP NF images (i.e., minimize [OSP1/m1] > [OSP2/m2] > [OSP3/m3] > [OSP4/m4]). Four non-saturated OSP NF beams are co-registered to ISP orientation to obtain a quad-averaged OSP beam, beam center, and the "top-map" of this beam. The 2D PSS correction is formed that minimizes individual beam peak/mean, where mean is of beam top and peak = Max(top) after smoothing with 1.5-cm scale. The PSS correction is extrapolated from the "top" of the quad-averaged beam out to the full extent of the OSP coordinates xOSP, yOSP using a radial zero-slope extrapolation method, and the result is smoothed over the entire array. An ISP coordinate system is defined of size ~2.2 cm based on the ISP cm/pixel. An ISP-to-OSP magnification M is derived in order to put the PSS correction array in the ISP frame via the pseudo-coordinates xOSP/M and yOSP/M (where M for the NIF is about 20.7). Then this correction is multiplied by a measured

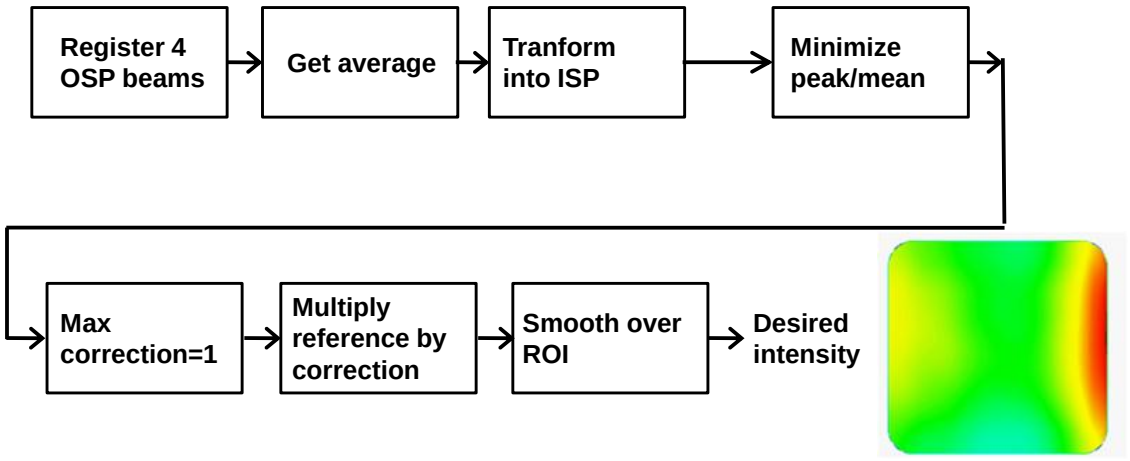

Figure 8. Process of generating the requested beam shape

"reference" regen beam to produce the "requested" regen shape that the PSS must make the laser obtain.

A regen beam is beam without any gain. This prefigure correction is saved in a file which is read by the PSS system. The block diagram in Fig. 8 depicts all these steps taken to generate a desired beam profile shown next to the output block.

To implement the spatial shaping at the PSS, the various steps taken are shown in Fig. 9. First, a reference beam with no pattern on the modulator is obtained. Then the requested pattern is divided by this new regen beam to obtain a PSS transmittance (prefigure). The transmittance is smoothed and extended to the full size of the LCOS to avoid the discontinuity in the beam edges. Then the gray level calibration data (S-curves) are utilized to map this into the gray levels necessary to obtain those transmission values. The correction gray levels are applied to the LCOS and a new beam image is captured in the ISP camera.

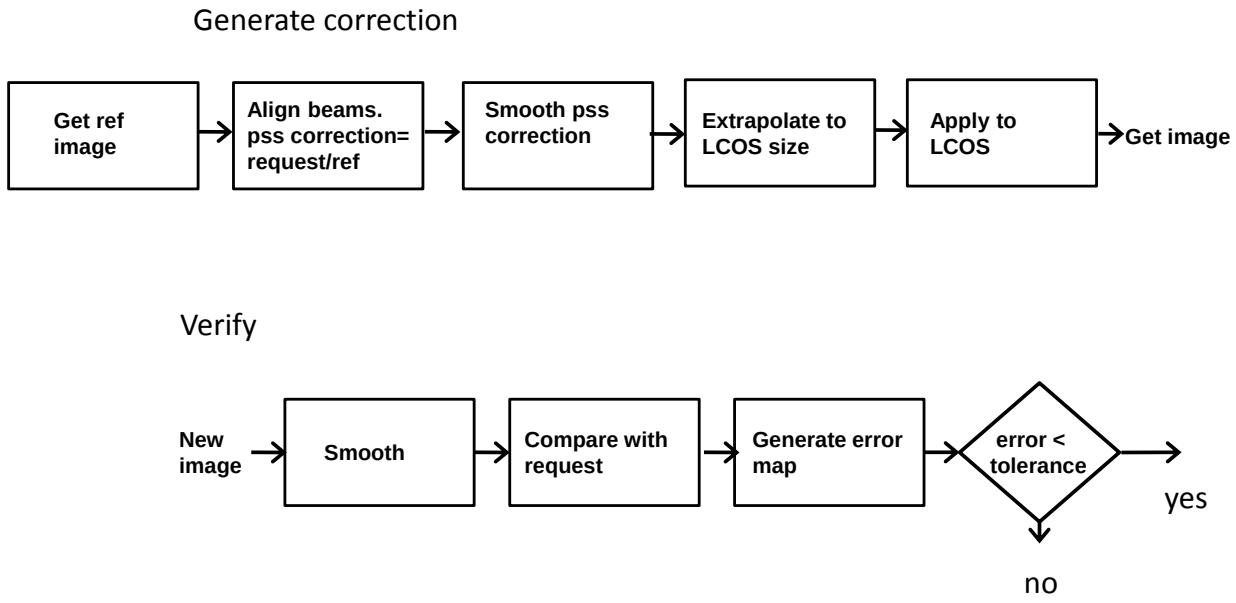

Figure 9. Process of implementing and verifying the requested beam shape

Next step is to verify that the desired intensity pattern was obtained as specified in the output block of Fig.8 . The new image obtained with that PSS prefigure emplaced is now compared with the requested LPOM beam profile after smoothing to see whether it is within some tolerance. The error map shown in lower left of Fig. 6 shows a typical output of this process. If the rms deviation is less than 3%, then it is considered within tolerance.

5. DISCUSSIONS

In this paper, the control system and underlying image processing required for deploying and verifying calibration blockers, gray blockers and overall beam spatial shapers are discussed. The software and the control systems were tested in the PSS development laboratory. The use of subimaging technique allowed for fast processing of images. The use of programmable spatial mask allows us to maximize the energy delivery to the target while maintaining reliability and flexibility of systems operation.

ACKNOWLEDGEMENTS

This work performed under the auspices of the U.S. Department of Energy by Lawrence Livermore National Laboratory under Contract DE-AC52-07NA27344. The authors acknowledge valuable comments made by Randy Roberts on this paper.

REFERENCES

1. E. I. Moses, "The National Ignition Facility: Status and Progress towards Fusion Ignition," Fusion Science and Technology, **61** (1T), 3-8 (2012).
2. E. Moses, "The National Ignition Facility: an experimental platform for studying behavior of matter under extreme conditions," Astrophysics and Space Science, **336(1)**, 3-7 (2011).
3. J. D. Lindl, L. J. Atherton, L. J. P. A. Amednt, et al., "Progress towards ignition on the National Ignition Facility," Nuclear Fusion, **51(9)** (2011).
4. J. V. Candy, W. A. McClay, A. A. S. Awwal, and S. W. Ferguson, "Optimal position estimation for the automatic alignment of a high-energy laser," Journal of Optical Society of America A, **22**, pp. 1348-1356, 2005.
5. R. A. Zacharias, N. R. Beer, E. S. Bliss, et al., "Alignment and wavefront control systems of the National Ignition Facility," Optical Engineering **43**, 2873-2884 (2004).
6. S. C. Burkhart, E. Bliss, P. Di Nicola, D. Kalantar, R. Lowe-Webb, T. McCarville, D. Nelson, T. Salmon, T. Schindler, J. Villanueva, K. Wilhelmsen, "National Ignition Facility system alignment," Appl. Opt., 50(8) 1136-1157 (2011)
7. K. Wilhelmsen, A. Awwal, W. Ferguson, B Horowitz, V. Miller Kamm, C. Reynolds, "Automatic Alignment System For The National Ignition Facility", Proceedings of 2007 International Conference on Accelerator and Large Experimental Control Systems (ICALEPCS07), 486-490, Knoxville, Tennessee (2007). http://accelconf.web.cern.ch/accelconf/ica07/PAPERS/ROAA02.PDF
8. J. Heebner, M. Borden, P. Miller, C. Stolz, T. Suratwala, P. Wegner, M. Hermann, M. Henesian, C. Haynam, S. Hunter, K. Christensen, N. Wong, L. Seppala, G. Brunton, E. Tse, A. Awwal, M. Franks, E. Marley, K. Williams, M. Scanlan, T. Budge, M. Monticelli, D. Walmer, S. Dixit, C. Widmayer, J. Wolfe, J. Bude, K. McCarty, and Jean-Michel DiNicola, "A Programmable Beam Shaping System for Tailoring the Profile of High Fluence Laser Beams," Boulder Laser damage conference, Boulder (2010).
9. M. Shaw, W. Williams, R. House, C. Haynam, "Laser performance operations model," Opt. Engg., **43(12)** 2885-2895 (2004).
10. M. Bowers, Scott Burkhart, Simon Cohen, Gaylen Erbert, John Heebner, Mark Hermann and Don Jedlovec, "The injection laser system on the National Ignition Facility", Proc. SPIE 6451, Solid State Lasers XVI: Technology and Devices, 64511M (2007);
11. Abdul A. S. Awwal, Richard Leach, Gordon Brunton, Eddy Tse, JoAnn Matone, John Heebner, "Image processing and control of a programmable spatial light modulator," Proc. SPIE. 7916, High Power Lasers for Fusion Research, 79160Q (2011).
12. A. VanderLugt, "Signal Detection by Complex Spatial Filtering", IEEE Trans. Inf. Theory **IT-10**, 139-145 (1964).
13. H. L. Van Trees, *Detection, Estimation, and Modulation Theory, Part I* (Wiley, 2001).
14. A. A. S. Awwal, Wilbert A. McClay, Walter S. Ferguson, James V. Candy, Thad Salmon, and Paul Wegner, "Detection and Tracking of the Back-Reflection of KDP Images in the presence or absence of a Phase mask," Applied Optics, **45**, 3038-3048 (2006).
15. Abdul A. S. Awwal, "Multi-object feature detection and error correction for NIF automatic optical alignment," Proc. of SPIE Vol. 6310, Photonic Devices and Algorithms for Computing VIII, 63100Q, (2006).
16. A. A. S. Awwal, Kenneth L. Rice, Tarek M. Taha, "Fast implementation of matched-filter-based automatic alignment image processing," Optics & Laser Technology **41**, 193-197 (2009).
17. M. A. Karim and A. A. S. Awwal, *Optical Computing: An Introduction*, John Wiley, New York, NY, 1992.
18. A. A. S. Awwal, "What can we learn from the shape of a correlation peak for position estimation?," Applied Optics, **49**, pp. B41-B50 (2010).
19. K. M. Iftekharuddin and Abdul A. Awwal, *Field Guide to Image Processing*, SPIE Field Guides, Volume FG25, SPIE Press, Bellingham, WA, 2012.